Pharm Res (2011) 28:1561–1576
DOI 10.1007/s11095-011-0389-6

RESEARCH PAPER

Pharmacokinetic-Pharmacodynamic Modeling of the Inhibitory Effects of Naproxen on the Time-Courses of Inflammatory Pain, Fever, and the *Ex Vivo* Synthesis of TXB_2 and PGE_2 in Rats

Elke H. J. Krekels • Marie Angesjö • Ingemo Sjögren • Kristina Ängeby Möller • Odd-Geir Berge • Sandra A. G. Visser

Received: 25 November 2010 / Accepted: 31 January 2011 / Published online: 23 February 2011

ABSTRACT

Purpose To quantify and compare the time-course and potency of the analgesic and antipyretic effects of naproxen in conjunction with the inhibition of PGE_2 and TXB_2.

Methods Analgesia was investigated in a rat model with carrageenan-induced arthritis using a gait analysis method. Antipyretics were studied in a yeast-induced fever model using telemetrically recorded body temperature. Inhibition of TXB_2 and PGE_2 synthesis was determined *ex vivo*. Pharmacokinetic profiles were obtained in satellite animals. Population PKPD modeling was used to analyze the data.

Results The IC_{50} values (95% CI) of naproxen for analgesia (27 (0–130) μM), antipyretics (40 (30–65) μM) and inhibition of PGE_2 (13 (6–45) μM) were in similar range, whereas inhibition of TXB_2 (5 (4–8) μM) was observed at lower concentrations. Variability in the behavioral measurement of analgesia was larger than for the other endpoints. The inhibition of fever by naproxen was followed by an increased rebound body temperature.

Conclusion Due to better sensitivity and similar drug-induced inhibition, the biomarker PGE_2 and the antipyretic effect would be suitable alternative endpoints to the analgesic effects for characterization and comparisons of potency and time-courses of drug candidates affecting the COX-2 pathway and to support human dose projections.

KEY WORDS analgesia · fever · naproxen · pharmacokinetic-pharmacodynamic modeling · prostaglandins

ABBREVIATIONS

COX	cyclooxygenase
CV%	coefficient of variation
LPS	lipopolysaccharide
NSAIDs	nonsteroidal anti-inflammatory drugs
PGE_2	prostaglandin E_2
TXB_2	thromboxane B_2

INTRODUCTION

At the end of the drug discovery phase, drug candidates are selected for further development that are expected to have the most favorable pharmacokinetic and pharmacodynamic profile in humans. The anticipated human efficacy profile is often based on data from preclinical models. To facilitate rational drug candidate selection, it is imperative to both characterize and quantify differences between the compounds and to quantify similarities and differences for the relevant efficacy endpoints between species to facilitate translation of preclinical findings to clinical efficacy (1–3).

Preclinical models that increase confidence of clinical efficacy are not always similar to models that give

E. H. J. Krekels • M. Angesjö • I. Sjögren • S. A. G. Visser (✉)
DMPK, CNSP iMed Science Södertälje, AstraZeneca Research and Development, Innovative Medicines
SE-151 85 Södertälje, Sweden
e-mail: Sandra.Visser@AstraZeneca.com

K. Ängeby Möller • O.-G. Berge
Neuroscience, CNSP iMed Science Södertälje
AstraZeneca Research and Development, Innovative Medicines
SE-151 85 Södertälje, Sweden

Present Address:
E. H. J. Krekels
Division of Pharmacology
Leiden/Amsterdam Center for Drug Research, Leiden University
Leiden, The Netherlands

detailed information on potency, intrinsic activity, time-course of the effect, and dose and time dependencies such as saturation, tolerance, and sensitization (1,4–6). With respect to *in vivo* pain models, it is challenging to differentiate compounds based on their analgesic efficacy due to substantial pharmacodynamic variability and limitations in measuring frequencies of both effect and exposure within an individual. Often, ED_{50} or minimal effective doses are reported, which ignores the pharmacokinetic properties of the compound, thereby complicating comparisons between compounds (3). It could therefore be useful to validate and characterize other endpoints that can be measured repeatedly with more sensitivity to allow for a quantitative differentiation of compounds. On the other hand, dose–response efficacy data in an animal pain model could increase the confidence in the translatability of other endpoints used for characterization, selection and dose predictions.

Non-steroidal anti-inflammatory drugs (NSAIDs) inhibit cyclooxygenase (COX) enzymes, preventing the conversion of arachidonic acid to various prostaglandins and thromboxanes. COX-1 is considered to be a housekeeping enzyme. COX-2 is best known for its local up-regulation by proinflammatory stimuli, its production of prostaglandins involved in inflammatory responses and its up-regulation in the spinal cord facilitating transduction of painful stimuli (7). Therefore, the analgesic and anti-inflammatory activity of NSAIDs is thought to be predominantly mediated through COX-2 inhibition (7–9).

Inhibition of *ex vivo* thromboxane B_2 (TXB_2) and prostaglandin E_2 (PGE_2) synthesis are biomarkers for COX-1 and COX-2 (in the presence of aspirin) activities, respectively (10–12). PGE_2 in the systemic circulation triggers the hypothalamus to elevate body temperature, resulting in a fever, which could also be regarded as an alternative endpoint for COX-2 activity.

Measurements of fever or *ex vivo* prostaglandin synthesis could be less variable and performed more frequently than behavioral pain readouts, and could therefore be potential alternative efficacy endpoints for the effects of drugs that affect the prostaglandin pathway. The use of the above endpoints in investigations of NSAIDs is not new (12–14); however, little is known about their temporal relationship with the pharmacokinetic profile. An investigation of the *in vivo* time-courses may give valuable information not only on the potency but also on possible dose and time dependencies. The aim of this study was therefore to characterize, quantify, and compare the time-course of the analgesic and antipyretic effects of naproxen in conjunction with the inhibition of TXB_2 and PGE_2 using a population pharmacokinetic-pharmacodynamic (PKPD) modeling approach.

MATERIALS AND METHODS

Table I summarizes the experimental design of the *in vivo* experiments.

Animals

Male Sprague–Dawley rats (Scanbur BK AB, Sollentuna, Sweden) were used in all five studies. Animals were housed in groups of 3–4 in transparent acrylic cages with wood shavings as bedding and with free access to food (DietLactamin R 70, Lactamin AB, Kimstad, Sweden) and tap water. Environmental conditions were 11.5 h light, 11.5 h dark, and 0.5 h for dusk and dawn, 20°C ± 2°C, and 40–80% relative humidity. Animals were acclimatized for a minimum of 1 week before they were subjected to experimental procedures. The experiments were approved by the Stockholm Södra Animal Research Ethical Board.

Drugs and Chemicals

Naproxen sodium, warfarin, aspirin, brewers' yeast, lambda carrageenan, lipopolysaccharide from E. coli (0111:B4 strain), acetic acid, and gelatin were purchased from Sigma-Aldrich (Stockholm, Sweden). Acetonitrile, ammonium acetate, heptane, hydrochloric acid, and methanol were obtained from Merck (Darmstad, Germany). Ethyl acetate was supplied by Fluka (Seelze, Germany), isoflurane by Abbott (Queensborough, UK), and pentobarbital by Apoteket (Stockholm, Sweden). All chemicals were of analytical grade.

Experimental Design

Study 1: Analgesic Effects of Naproxen in a Carrageenan-Induced Model of Monoarthritis

Animals (n=48, 217 ± 28 g) were randomly divided into four groups of 12 by an internally developed computer program, allowing the blind performance of the behavioral experiment.

To induce hyperalgesia by inflammation, animals in groups 1B, 1C, and 1D received a 40-μL intra-articular injection of a saline solution containing 7.5 mg/mL carrageenan in the left hind limb under isoflurane anesthesia (time = −1 h). Animals in group 1A received no injection. After 1 h (time = 0) the animals in groups 1A, 1B, 1C, and 1D received oral doses of naproxen in saline of 0, 0, 7.5 and 30 μmol/kg, respectively. The doses and time points of measurements were selected on the basis of simulations predicting measuring a full concentration-effect relationship within the time-span of the experiment.

Table I Overview of the Experimental Design

Group	Number of animals	Agent of disease induction	Naproxen dose (μmol/kg)	Types of measurements and time points of collecting these measurements
Study 1: Antinociception in carrageenan-induced monoarthritis				
1A	12	–	0	Guarding index: Subgroups of $n=4$:
1B	12	Carrageenan	0	i) −2, 0.5, 2, 4, 7, and 23.5 h
1C	12	Carrageenan	7.5	ii) −2, 1, 3, 5, 6, and 24 h
1D	12	Carrageenan	30	iii) −2, 1.5, 17, 19, 21, and 23 h
				Naproxen concentration: 25 h
1SA	3	–	0	Naproxen concentration: 1, 3, 5, and 25 h
1SB	3	Carrageenan	0	*Ex vivo* TXB_2 synthesis: 25 h
1SC	3	Carrageenan	7.5	
1SD	3	Carrageenan	30	
Study 2: TXB_2 synthesis in carrageenan-induced monoarthritis[a]				
2A	3	Vehicle	0	*Ex vivo* TXB_2 and PGE_2 synthesis & naproxen concentration: 1 h (group 2A), 0.5, 1.5, 3, 5, 7, 17,
2B	24	Carrageenan	0	20, or 24 h (groups 2B, 2C, and 2D, $n=3$ per group per time point)
2C	24	Carrageenan	7.5	
2D	24	Carrageenan	30	
Study 3: Antipyretics in brewers'yeast-induced fever				
3A	6	Vehicle	0	Fever: continuous measurements between −1 and 3 days after yeast injection.
3B	6	Yeast	0	
3C	6	Yeast	7.5	
3D	6	Yeast	15	
3E	6	Yeast	30	
3F	6	Yeast	90	
3SA	6	Vehicle	30	Naproxen concentration: Subgroups of $n=3$:
3SB	6	Yeast	30	i) 1, 2, 3.5, 5 and 25 h
				ii) 0,5, 16, 18, 20, and 22 h
Study 4: PGE_2 in brewers' yeast-induced fever				
4A	6	Vehicle	0	*Ex vivo* PGE_2 synthesis & naproxen concentration: Subgroups of $n=3$ for 4A, 4B, 4C, 4E, and 4F:
4B	6	Vehicle	7.5	i) −0.5, 1, 17 and 21 h
4C	6	Vehicle	30	ii) −0.5, 3, 5 and 25 h
4D	6	Vehicle	90	and subgroups of $n=3$ for 4D:
4E	6	Yeast	0	iii) −0.5, 17, 21, and 42 h
4F	6	Yeast	30	iv) −0.5, 1, 5, and 25 h
Study 5: Correlation between TXB_2 and PGE_2 synthesis in naive animals				
5A	2	–	0	*Ex vivo* TXB_2 and PGE_2 synthesis & naproxen concentration: 3 h
5B	2	–	0.5	
5C	2	–	1	
5D	2	–	2	
5E	2	–	7.5	
5F	2	–	30	
5G	2	–	90	

[a] Samples for PGE_2 analysis were taken, but analysis failed in incubation step with LPS

1SA-1SD and 3SA and 3SB are satellite PK groups

A maximum of six behavioral pain measurements were performed per animal. To obtain measurements over a large part of the time-effect curve, each group of 12 animals was further divided into three subgroups of four animals in which pain behavior was measured at times a) –2, 0.5, 2, 4 7, 23.5 h; b) –2, 1, 3, 5, 6, 24 h, or c) –2, 1.5, 17, 19, 21, 23 h. Blood samples to determine naproxen concentrations could not be obtained during the behavioral experiment and were only obtained at the end of the experiment (time = 25 h) via heart puncture under isoflurane anesthesia. The animals were then sacrificed by an overdose of pentobarbital while anesthetized.

Naproxen pharmacokinetics were determined in 12 satellite animals (240 ± 14 g), which were randomly divided into four groups (1SA–1SD), all receiving intra-articular carrageenan injections and oral naproxen doses identical to the animals in groups 1A–1D. Three blood samples were taken from the tail vein at 1, 3, and 5 h, and one blood sample was taken at the end of the experiment (time = 25 h) by heart puncture. In the last sample, inhibition of *ex vivo* TXB_2 synthesis was also determined. Animals were sacrificed by an overdose of pentobarbital while anesthetized.

The PawPrint set-up, an internally developed computer system based on the same gait analysis concept as the CatWalk method described by Vrinten and Hamers (15), was used in the behavioral pain measurement (16). Briefly, the PawPrint set-up consists of a 100 × 10 cm pathway which rats are trained to traverse in a continuous passage on three or four separate training occasions before the experiment. The walkway has a glass floor into which light is projected via fiber optics. This light is almost completely reflected internally. When an object, such as a rat limb, touches the glass, the light is scattered at the point of contact, resulting in an illuminated print. The area and light intensity of this print increase with increased pressure. A wide-angle camera placed under the walkway records the print, and a computerized gait detection algorithm subsequently extracts several parameters pertaining to the gait pattern and weight bearing from the prints.

Nociception as a result of the induced hyperalgesia was defined in terms of a guarding index as the difference in weight bearing between the hind paws (in per mill (‰) of total weight bearing on all limbs). A guarding index of 0 indicates that there is an equal amount of weight bearing on the left and the right hind paw. An increase in the guarding index indicates a shift of weight bearing from the affected left paw to the unaffected right paw.

Study 2: Ex Vivo TXB_2 Synthesis in Carrageenan-Induced Model of Monoarthritis

Animals (n = 75, 236 ± 12 g) were randomly divided into four groups (2A–2D). Similar to study 1, at time = −1 h animals in groups 2B, 2C, and 2D (n = 24 in each group) received a 40-μL intra-articular injection of a saline solution containing 7.5 mg/mL carrageenan under isoflurane anesthesia. The animals in group 2A (n = 3) received no injection. One hour after the injection (time = 0 h), the animals in groups 2A, 2B, 2C, and 2D received oral doses of naproxen in saline of 0, 0, 7.5 and 30 μmol/kg, respectively. Blood samples were obtained by heart puncture under isoflurane anesthesia and immediately divided into aliquots for the analysis of naproxen concentrations and of the *ex vivo* synthesis of TXB_2. In groups 2B, 2C, and 2D, blood samples were taken at time 0.5, 1.5, 3, 5, 7, 17, 20, or 24 h (n = 3 per group per time point). For animals in the vehicle group (2A), this sample was taken shortly after dosing. The animals were sacrificed by an overdose of pentobarbital while anesthetized.

Study 3: Antipyretics in a Brewers' Yeast-Induced Fever Model

Animals (n = 36, 327 ± 33 g) were randomly divided into six groups of six. At time = −4 h animals in groups 3B, 3C, 3D, 3E, 3F received a 2 g/kg s.c. injection of brewers' yeast in saline (0.2 g/mL) under isoflurane anesthesia to induce fever. Animals in group 3A received a sham injection. Four hours later (time = 0) the animals in groups 3A, 3B, 3C, 3D, 3E, and 3F received oral doses of naproxen in saline of 0, 0, 7.5, 15, 30, and 90 μmol/kg, respectively. The doses were selected on the basis of simulations predicting measuring a full concentration-effect relationship within the time-span of the experiment.

Twelve satellite animals (263 ± 8 g) were randomly divided into two groups of six (3SA and 3SB) to determine the pharmacokinetics. The animals in group 3SB received an s.c. brewers' yeast injection, while the animals in group 3SA received a sham injection at time = −4 h. Four hours later, the animals in both groups received an oral dose of 30 μmol/kg naproxen. Both groups were divided into two subgroups (n = 3), and blood samples to determination naproxen concentrations were taken via the tail vein at times a) 1, 2, 3.5, 5, or 25 h or b) 0.5, 16, 18, 20, and 22 h.

Body temperature in the animals of groups 3A–3F was measured by a temperature transmitter (TA10TA-F20, Data Sciences, St Paul, Minn., USA) that had been implanted intra-abdominally under isoflurane anesthesia 3 days before the start of the experiment. The peritoneal cavity was closed with a normal suture and cleaned with saline. The animals were housed individually after the surgery.

Body temperature was recorded 1 day prior to dosing until 3 days after dosing. The telemetry signals were measured every 5 min for a 10-s period and signaled to a receiver. Using the software package Dataquest ART 2.2 (Data Sciences), the

temperature data were processed. The animals were disturbed as little as possible throughout the experiment. At the end of the experiment the animals were sacrificed by an overdose of pentobarbital while anesthetized.

Study 4: PGE_2 Synthesis in a Brewers' Yeast-Induced Fever Model

Animals ($n=36$, 273 ± 16 g) were randomly divided into six groups of six (4A–4F). At time $=-4$ h animals in groups 4A, 4B, 4C, and 4D received a sham injection, and animals in groups 4E and 4F received a 2 g/kg s.c. injection of brewers' yeast in saline (0.2 g/mL) under isoflurane anesthesia. Four hours after the injection (time $=0$) animals in groups 4A, 4B, 4C, 4D, 4E, and 4F received oral doses of naproxen in saline of 0, 7.5, 30, 90, 0, and 30 μmol/kg, respectively. Each group was subdivided into two groups of three in which blood samples to determine naproxen concentrations and *ex vivo* synthesis of PGE_2 were taken via the tail vein at times a) −0.5, 1, 17, and 21 h or b) −0.5, 3, 5, and 25 h, except for group 4D, where blood was collected at time c) −0.5, 17, 21, and 42 h and d) −0.5, 1, 5, and 25 h. At the end of the experiment the animals were sacrificed by an overdose of pentobarbital while anesthetized.

Study 5: Correlation Between TXB_2 and PGE_2 Synthesis in Naive Animals

Animals ($n=14$, 288 ± 11 g) were randomly divided into seven groups of two (5A–5G) and given oral doses of naproxen in saline of 0, 0.5, 1, 2, 7.5, 30, and 90 μmol/kg, respectively, at time $=0$ h.

After 3 h, a blood sample was obtained from each animal by heart puncture under isoflurane anesthesia and immediately divided into aliquots for the analysis of naproxen concentrations and of the *ex vivo* synthesis of TXB_2 and PGE_2. The animals were sacrificed by an overdose of pentobarbital while anesthetized.

Analysis of Blood Samples

Naproxen Concentration

Blood was collected in EDTA tubes (BD Microtainer tube). All samples were centrifuged at 3,000 rpm for 10 min at 4°C. Plasma was stored at −80°C until analysis. At time of analysis, a cold mixture of acetonitrile/water (50/50 v/v) was added to the plasma samples to precipitate proteins. The supernatant was diluted with mobile phase and injected into the LC system. Calibration solutions and quality controls were prepared and added to blank plasma. Warfarin served as the internal standard.

The LC-system was a reversed-phase system HTLC 2300 (Cohesive Technologies, Crownhill, UK) with a Zorbax extend C_{18} 5 μm trap column, 12.5×2.1 mm i.d. (Agilent Technologies, Scantec lab, Partille, Sweden). Chromatographic separation was performed on an Atlantis C_{18} 3 μm column, 30×2.1 mm i.d. (Waters, Dublin, Ireland). The mobile phase consisted of A: 2.0% ACN in 0.1% HAc and B: 80% ACN in 0.1% HAc in a gradient cycle of 1 min in a composition of 99% A and 1% B followed by a 3.5 min composition of 35% A and 65% B. The flow rate remained 0.35 mL/min throughout the cycle.

Mass detection was carried out on a Quattro Ultima™ mass spectrometer with an electrospray source (Micromass Ltd., Altrincham, UK), which was directly coupled to the LC system. Analytes were ionized in the negative mode. The scan mode was multiple reaction monitoring (MRM), the MRM transitions being m/z $229\rightarrow185$ for naproxen and m/z $307\rightarrow161$ for warfarin. MS/MS control, data acquisition, and data processing were performed using MassLynx 3.4 software (Micromass Ltd., Altrincham, UK). The limit of quantification was 0.32 μM based on a 20 μl sample. Accuracy was between 84% and 103%, precision ranged between 4.5% and 8.4%, and reproducibility was between 6% and 13%.

Ex Vivo TXB_2 and PGE_2 Synthesis

Blood samples for the determination of *ex vivo* TXB_2 synthesis were collected in glass tubes and incubated for 1 h$\pm$2.5 min at 37°C. All samples were centrifuged at 3,000 rpm for 10 min at 4°C. Serum from these samples was stored at −80°C until analysis. Blood samples for the determination of *ex vivo* PGE_2 synthesis were collected in lithium heparinized tubes (BD Microtainer tube), to which 5 μl of a 1 mg/ml aqueous aspirin solution was added to inactivate the COX-1 pathway. After 45 min, 5 μl of a 1 mg/ml LPS solution in saline was added. This was incubated for 24 h under an atmosphere of 5% CO_2 and 95% air at 37°C. All samples were centrifuged at 3,000 rpm for 10 min at 4°C. Supernatant was subsequently stored at −80°C until analysis.

The concentrations of synthesized TXB_2 in the incubated serum samples were determined with a Biotrak thromboxane B_2 enzyme immunoassay kit (GE Healthcare, Amersham, Buckinghamshire, UK). The concentration of synthesized PGE_2 in the plasma samples of was determined by a Prostaglandin E_2 Biotrak enzyme immunoassay kit (GE Healthcare, Amersham, Buckinghamshire, UK). Analysis of *ex vivo* PGE_2 synthesis in study 2 failed in the incubation step.

All kits were based on the same principle. Briefly, the plasma samples were diluted with provided assay buffer and added to an antibody-coated plate. Antiserum and/or an enzyme conjugate were added and incubated at room

temperature. The plate was subsequently washed with provided buffer solution after which the enzyme substrate was added. After a second incubation step, the enzyme reaction was halted, and light absorption at 450 nm for TXB_2 or optical density at 450 nm for PGE_2 was measured in a microplate reader (Spectramax 340, Molecular Devices, Sunnyvale, USA). Data acquisition and processing were performed using SOFTmax PRO 4.3 Software (Molecular devices, Sunnyvale, USA). Standard solutions were prepared in the assay buffer solution from a stock vial provided in the kit.

The intra-day precision was generally well below 20% for PGE2 and for TXB2 below 15%, with a few samples ranging up to 25%. Inter-day variability (reproducibility) ranged between 7% and 14%. All samples were run in duplicate. Concentration values were accepted when they were within the calibration curve with a variation of less than 25% or else rerun.

Pharmacokinetic-Pharmacodynamic Data Analysis

All the data were analyzed using a population approach based on non-linear mixed-effect modeling using the NONMEM software package (Version VI, Globomax, USA). The ADVAN6 TOL5 subroutine and the FOCE interaction method were used unless stated otherwise.

Model selection was based on visual inspection of the goodness-of-fit plots, on the parameter estimates and their confidence interval, and on the minimum value of objective function. For the visual predictive checks, 1,000 simulations were performed in Berkeley Madonna 8.3.9 (http://www.berkeleymadonna.com), and the mean predictions ±2*SD were used as an approximation of the 95% prediction interval.

Modeling of Pharmacokinetics

Naproxen concentrations from all five experiments were fitted simultaneously to a standard two-compartment pharmacokinetic model with first-order absorption. The inter-individual variability of all estimated parameters was modeled by an exponential equation. The administration of yeast was investigated as a covariate for naproxen clearance.

For the pharmacodynamic modeling of the antinociceptive effect, individual pharmacokinetic *post hoc* parameter estimates were obtained from each animal based on the blood sample taken after the pharmacodynamic measurements. These *post hoc* parameters were used to calculate the plasma concentrations at the times of the pharmacodynamic measurements for each individual animal in the pharmacodynamic experiment. Since no blood samples were obtained from animals in the fever study, population parameter estimates were used to calculate plasma concentrations at the times of the pharmacodynamic measurements. As both *ex vivo* biomarker synthesis and naproxen concentrations were measured in the same samples, the actual measured naproxen concentrations were used in the pharmacodynamic modeling of the biomarkers.

Modeling of the Analgesic Effects

The effect of carrageenan on the guarding index was time-dependent. This time-course was described by a modified Bateman function (17):

$$GI_{DP} = GI_{BL} + \left(a_1 \cdot e^{(-b_1 \cdot time)} - a_2 \cdot e^{(-b_2 \cdot time)}\right) \quad (1)$$

In this equation, GI_{DP} represents the disease progression of the guarding index; GI_{BL} represents the guarding index when no inflammation is present; a_1, a_2, b_1, and b_2 represent coefficients that are estimated to obtain the best fit to the data; and *time* represents the time in hours after carrageenan administration.

The analgesic effect ($E_{analgesic}$) of naproxen on the guarding index was defined by a standard sigmoidal I_{max} model:

$$E = 1 - \frac{I_{\max} \cdot C_p{}^n}{IC_{50}{}^n + C_p{}^n} \quad (2)$$

where I_{max} is the maximal inhibition which was fixed to 1, thereby assuming that naproxen can fully inhibit the disease progression in the guarding index. IC_{50} is the naproxen concentration at which 50% of the maximum inhibition is reached, also known as the potency, and n is the hill-factor which was also fixed to 1. The time-course of changes in guarding index therefore was defined as

$$GI = GI_{DP} \cdot E_{analgesia}. \quad (3)$$

The data were analyzed in a two-step approach in which first the disease progression was fitted and in the subsequent analysis the drug effects, while fixing the parameters describing the disease progression. This was necessary due to the large variability in the data. In both analyses, the PRED subroutine was used. A constant coefficient of variation model was used to describe the inter-individual variability of the parameters b_1 and b_2. An additive error model was used to parameterize the inter-individual variability of IC_{50} values. A constant coefficient of variation model was used to describe the residual error.

Modeling of the Antipyretic Effects

In this analysis, the temperature data were used as absolute values. The circadian rhythm in the body

temperature ($T_{circadian}$) was described using the following equation:

$$T_{circadian} = T_{ref} \cdot (1 - amp \cdot \sin(2 \cdot \pi / period \cdot t)) \quad (4)$$

where T_{ref} is the reference temperature level, *amp* adjusts the amplitude of the circadian rhythm, and *period* stands for the 24 h period.

An empirical handling function *HF* was used to describe the transient increase in body temperature due to handling for yeast/sham injection (HF_{yeast}) or drug/vehicle administration (HF_{drug}) (18):

$$HF = 1 + k_{HF} \cdot (t - t_{HF}) \cdot p_{HF} \cdot e^{-k_{HF} \cdot (t - t_{HF})} \text{ when } t > t_{HF} \quad (5)$$

where k_{HF} determines the rate of the appearance and disappearance of the transient temperature elevation, and p_{HF} determines the magnitude of the temperature elevation, while t_{HF} is set to the time of handling. The baseline temperature profile (T_{BL}) in group 3A was then defined as

$$T_{BL} = T_{circadian} \cdot HF_{yeast} \cdot HF_{drug}. \quad (6)$$

The effect of yeast on the body temperature was time-dependent with an initial decrease, followed by an increase of up to 4 h and a subsequent slow decline towards baseline. The time-course of fever (T_{DP}) in group 3B was parameterized using the modified Bateman function (17):

$$T_{DP} = T_{LOW} \cdot HF_{yeast} \cdot HF_{drug} \cdot \left(1 + a_1 \cdot e^{-b_1 \cdot time} - a_2 \cdot e^{-b_2 \cdot time}\right) \quad (7)$$

In this equation, a_1, a_2, b_1, and b_2 represent the coefficients that are estimated to give the best fit to the data. T_{LOW} represents the lowest temperature reached after yeast administration, and *time* represents the time in hours after yeast injection.

To account for the observed tolerance and rebound, the effect of naproxen on fever in groups 2C–2F was described using a precursor-dependent indirect response model to account for the observed tolerance and rebound (19):

$$\begin{cases} d/dt(R) = k_p \cdot P \cdot E_{antipyretic} - k_{out} \cdot R \\ d/dt(P) = k_{in} - k_p \cdot P \cdot E_{antipyretic} \end{cases} \quad (8)$$

with initial conditions being

$$\begin{cases} P_0 = \frac{k_{in}}{k_p} \\ R_0 = k_p \cdot \frac{P_0}{k_{out}} = \frac{k_{in}}{k_{out}} \end{cases} \quad (9)$$

in which P is the precursor of the response, R is the response, k_{in} is the zero-order production rate of the precursor, k_{out} is the first-order loss rate constant for the response and k_p is the first-order rate constant by which the precursor is converted into the response. The response at time 0 (R_0) was fixed at 1, leading to that $k_{in} = k_{out}$ and thereby reducing the number of parameters.

The effect of naproxen on fever ($E_{antipyretic}$) was described by a sigmoidal I_{max} equation (Eq. 2) in which the I_{max} was fixed to 0.04, corresponding to the maximal possible decrease from the elevated body temperature back to the untreated level, which was 1.5°C. The time-course of body temperature (T) in the animals in groups 3C–3F was defined as

$$T = T_{DP} \cdot R \quad (10)$$

The model was developed by analyzing T_{BL}, T_{DP}, and T in a sequential way, but in the final analysis a two-step approach was used. In the first step, the T_{BL} and T_{DP} were fitted simultaneously using the PRED subroutine, and in the second step the drug effects were fitted using the ADVAN6 subroutine, while fixing T_{BL} and T_{DP}. This was done to avoid long run times. Inter-individual variability in the values of k_{htf} a_1, a_2, b_1, b_2, IC_{50} and k_{out} was best described by an exponential error model and for T_{ref}, *amp*, p_{HF} and T_{low} by a constant coefficient of variation model. The residual error in both analyses was described with an additive model.

Modeling of the TXB_2 and PGE_2 Biomarkers

The decrease from baseline of the *ex vivo* synthesized TXB_2 and PGE_2 was described with a sigmoidal I_{max} model (Eq. 2). The maximum decrease (I_{max}) was fixed to 1 for TXB_2 thereby assuming that naproxen can fully inhibit *ex vivo* TXB_2 synthesis, but was estimated for PGE_2. As for TXB_2, only single observations per animal were available; no inter-individual variability could be estimated. For PGE_2, exponential error models were used to describe the inter-individual variability in baseline value, I_{max}, and IC_{50}. Residual error was modeled with a constant coefficient of variation model.

RESULTS

Pharmacokinetics

A two-compartment model with first-order absorption described the time-course of naproxen plasma concentrations best in all studies. Yeast-induced fever was found to reduce naproxen clearance by 24%. Obtained pharmacokinetic parameter estimates are given in Table II. Fig. 1 depicts the population-predicted concentration and the 95% prediction interval for the naproxen concentrations with (blue) and without (red) fever of the three naproxen dose levels in studies 1, 2, 3 and 4.

Table II Population Pharmacokinetic Parameter Estimates for Naproxen

Parameter	Unit	Estimate	CV (%)	Inter-individual variability (%)
Cl/F (no fever)	$L \cdot h^{-1} \cdot kg^{-1}$	0.031	8	15
Cl/F (fever)	$L \cdot h^{-1} \cdot kg^{-1}$	0.024	47	15
K_a	h^{-1}	0.54	27	4
V_1/F	$L \cdot kg^{-1}$	0.016	39	–
Q	$L \cdot h^{-1} \cdot kg^{-1}$	0.15	38	–
V_2/F	$L \cdot kg^{-1}$	0.16	12	–

Residual variability was 41%

K_a absorption rate constant, *CL/F* apparent clearance, *Q* inter-compartmental distribution, V_1/F and V_2/F the apparent volumes of the central and peripheral compartment, *CV* coefficient of variation

Analgesic Effects

Six pain measurements were obtained from each of the 48 rats, and a large inter- and intra-individual variability was observed. However, mean guarding index profiles in Fig. 2 clearly show that the induction of monoarthritis by an intra-articular carrageenan injection at time = −1 h caused, after a delayed onset, a steep increase in the guarding index, indicating an increased weight bearing on the unaffected right hind limb compared to the affected left one. Between 3 and 8 h, the guarding index was relatively constant around 375‰, after which it declined to approx. 200‰ at 25 h. Fig. 2 also shows that the oral administration of naproxen at time = 0 dose-dependently decreased the guarding index, indicating a reversal of the disease-induced weight shift to the unaffected hind limb.

The time-course in the guarding index (GI_{DP}) as a result of an intra-articular injection of carrageenan (group 1A and 1B) was described with a modified Bateman function (Eq. 1), with an intra-individual variability of 69%. Different values were estimated for a_1 and a_2 to describe the delay in the onset of this profile. This function estimated the guarding index to be at maximum between 3 and 15 h after the injection of carrageenan.

Naproxen reduced the guarding index induced by carrageenan. Different drug effect models (direct and indirect) were investigated to describe the effect, but it was not possible to discriminate the performance of different models due to the large variability. Therefore, a standard sigmoidal I_{max} model was used, in which I_{max} and n were fixed to 1. All estimated parameters are listed in Table III. In Fig. 3, the population predictions and 95% prediction intervals of the guarding index are shown for each treatment group in study 1. The large residual variability (130%) and inter-individual variability for IC_{50} (120%) and the broad prediction intervals in Fig. 3 indicate that the results of this analysis should be interpreted cautiously.

Antipyretic Effects

The mean temperature profiles in Fig. 4 show a clear circadian variation in the naive animals with body temperatures close to 38°C during the nighttime and close to 37°C during the daytime. Handling of these animals for dosing

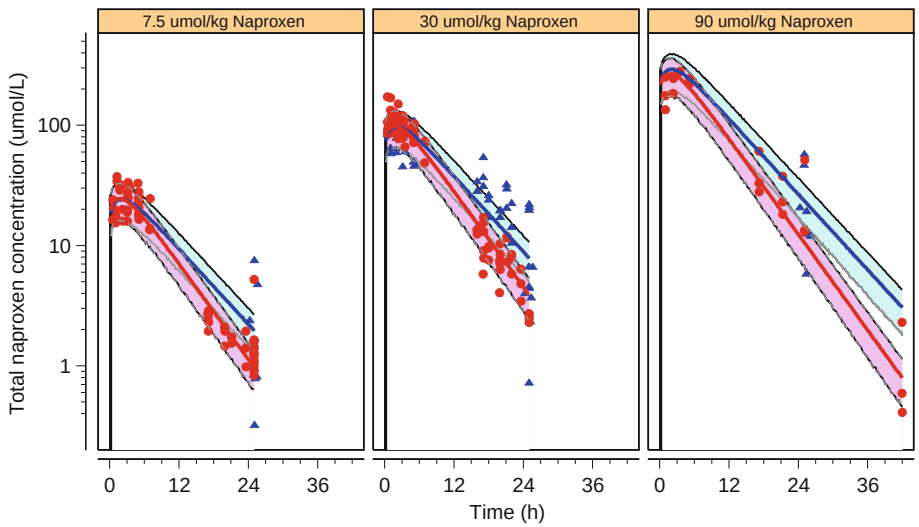

Fig. 1 Individually observed plasma concentrations after oral dosing of 7.5, 30, and 90 μmol/kg naproxen with the population prediction and the 95% prediction interval after 1,000 simulations in the absence (●, *red line* and area) and presence (▲, *blue line* and area) of brewers' yeast.

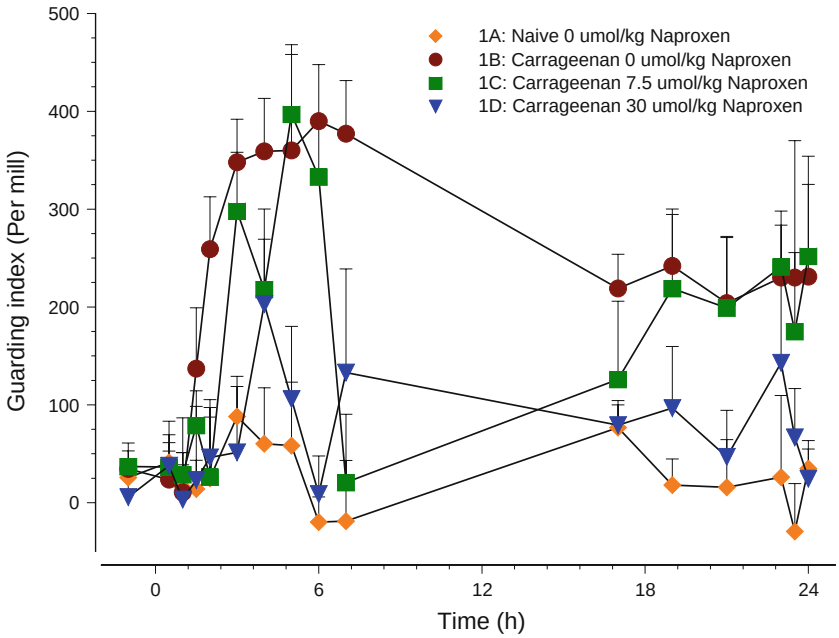

Fig. 2 The time-course of the guarding index in study 1 (mean ± SE, $n = 3$–4 per treatment per time-point). Carrageenan or vehicle injection occurred at time = −1 h, oral naproxen or placebo administration at time = 0 h.

purposes caused a transient increase in body temperature. Yeast administration at time = −4 caused a rapid initial decline in body temperature to 36°C, followed by an increase to 39°C 4 h later. Compared to the naive temperature profile, the temperature elevation was relatively constant during the first 20 h, after which it gradually declined. Thirty-four hours after the yeast injection, the body temperature overlapped with the naive group again during the nighttime, although the temperature during the daytime was still slightly higher than control, up to 60 h after yeast injection.

Also shown in Fig. 4 is that naproxen dose-dependently prevented the yeast-induced elevation in body temperature during the first 20 h after naproxen dosing. This was followed by an increase in body temperature higher than the vehicle-treated rats (rebound), which was more pronounced at higher doses. The area under the effect curve and the area under the rebound phase were similar, and the precursor-dependent indirect response model was therefore used to model the effect of naproxen on yeast-induced fever. Since the rebound phase for the highest dose lasted longer than the fever in the saline group, it was not possible to make use of baseline temperatures to rescale temperature for estimation of the relative drug effect and by that means reduce the number of parameters (18).

In Fig. 5 the observations, population predictions, and 95% prediction intervals are plotted for each treatment

Table III Population Pharmacodynamic Parameter Estimates for Disease Progression of Carrageenan-Induced Guarding Index and the Analgesic Effects of Naproxen

Parameter	Unit	Estimate	RSE (%)	Inter-individual variability (%)
GI_{BL}	‰	27	40	80
a_1	–	347	20	18
a_2	–	945	26	21
b_1	–	0.021	26	–
b_2	–	0.58	18	–
I_{max}	‰	1 fixed	–	–
IC_{50}	μM	27	34	120
n	–	1 fixed	–	–

Residual variabilities for disease progression (GI_{DP}) and final drug effect analysis (GI) were 69% and 130%, respectively

Explanations of the symbols can be found in Eqs. 1 and 2 in "Modeling of the Analgesic Effects"

RSE relative standard error of estimate

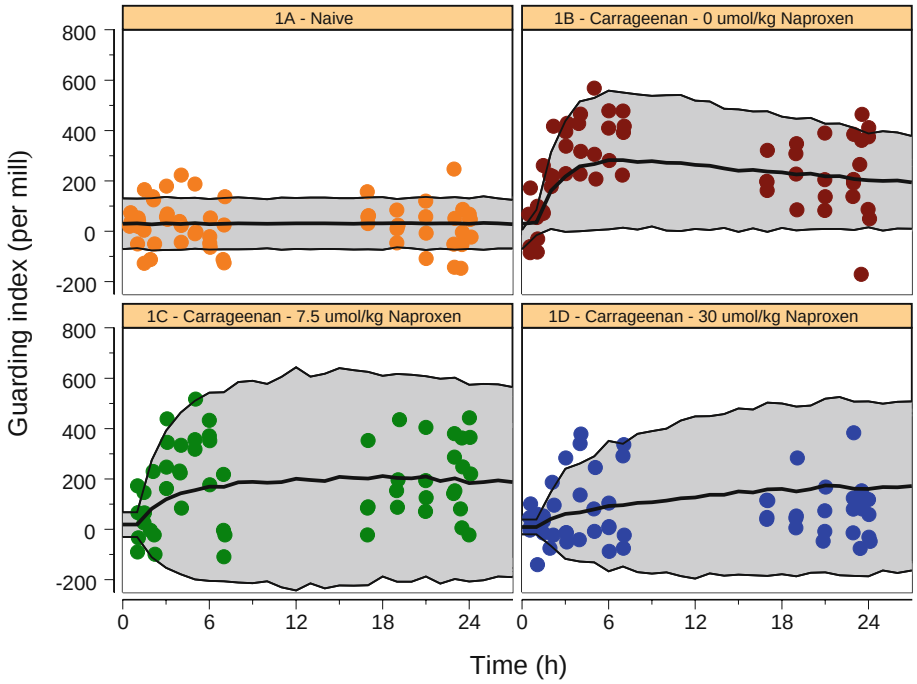

Fig. 3 Individually observed guarding indices in naive animals and after oral dosing of 0, 7.5, and 30 μmol/kg naproxen in the presence of carrageenan with population prediction (*thick line*) and the 95% prediction interval (*thin lines*) after 1,000 simulations (groups 1A, 1B, 1C, and 1D, respectively).

group in study 3. All parameter estimates are listed in Table IV.

Inhibition of *Ex Vivo* Synthesis of the Biomarkers TXB_2 and PGE_2

Figs. 6 and 7 show individually observed concentrations (dots), population predictions, and 95% prediction intervals (thick and thin lines) of *ex vivo* synthesized PGE_2 and TXB_2, respectively. Fig. 6 shows that the intra-articular carrageenan injection had no effect on the *ex vivo* formation of TXB_2 compared to naive animals. Therefore, data from studies 2 and 5 were pooled. In study 4, it was observed that the subcutaneous injection of brewers' yeast had no effect on the LPS-induced PGE_2 concentrations (data not shown). Therefore, PGE_2 data from studies 4 and 5 were also pooled.

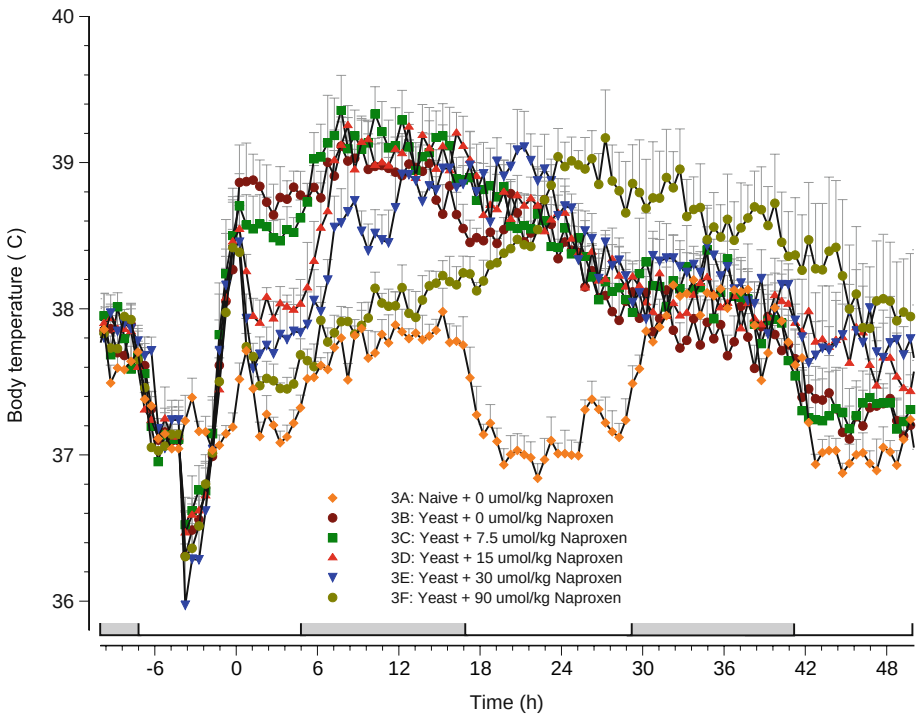

Fig. 4 The time-course of body temperature (°C) in study 3 (mean ± SE, $n = 6$ per group). Yeast or vehicle injection was given at time = −4 h, oral naproxen or placebo administration at time = 0 h. Daytime is between −7–5 h, 17–29 h and after 41 h. Nighttime is between 5–17 h and 29–41 h.

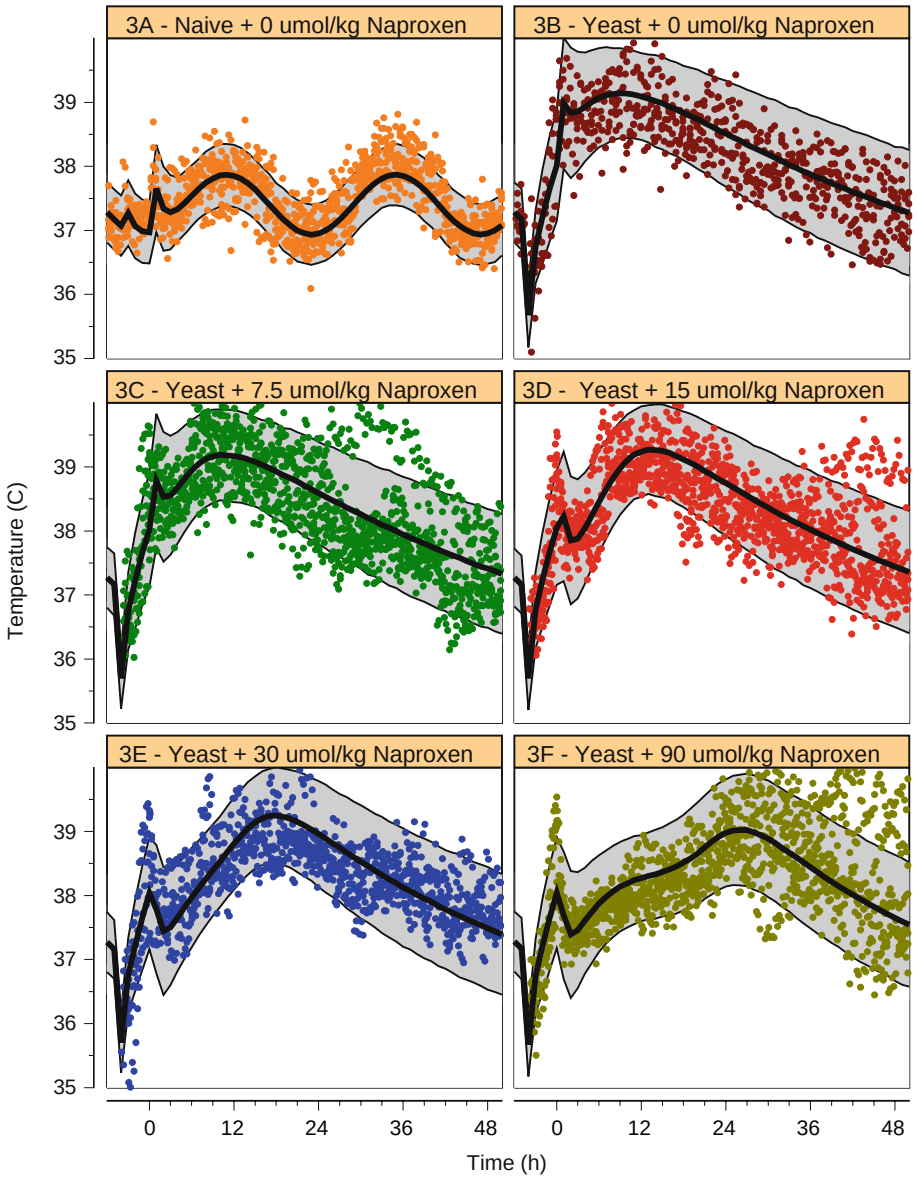

Fig. 5 Individual observed temperatures (°C) after administration of yeast or saline (time = −4 h) and oral dosing of 0, 7.5, 15, 30, and 90 μmol/kg naproxen at time = 0 h with population predictions (*thick line*) and the 95% confidence interval of the predictions (*thin black lines*) after 1,000 simulations.

The inhibitory effect of naproxen on LPS-induced PGE_2 synthesis and the platelet-derived TXB_2 synthesis was fitted to a sigmoidal I_{max} model. The parameter estimates are listed in Table V. Estimation of I_{max} for PGE_2 inhibition improved goodness of fit and significantly decreased objective function.

Comparisons

In Fig. 8, the population prediction and the 95% confidence interval after 1,000 simulations are shown for the four studied endpoints: analgesia, antipyretics, inhibition of *ex vivo* PGE_2 and TXB_2 synthesis. The IC_{50} values and the corresponding 95% confidence intervals for naproxen on the analgesia (27 (0–130) μM), antipyretics (40 (30–65) μM) and inhibition of *ex vivo* PGE_2 synthesis (13 (6–45) μM) are in a similar range, whereas naproxen inhibition of *ex vivo* TXB_2 synthesis at lower concentrations (5 (4–8) μM). There is a large difference in confidence intervals between the various endpoints, which were wide for the analgesic measurements, moderate for the inhibition of PGE_2 synthesis and antipyretic measurements, and narrow for the inhibition of TXB_2 synthesis.

DISCUSSION

In the present investigation the time-courses of the analgesic and antipyretic effects of naproxen in conjunction with the inhibition of the prostaglandins PGE_2 and TXB_2 were characterized and quantified using a population PKPD modeling approach.

Table IV Population Pharmacodynamic Parameter Estimates for the Disease Progression of Yeast-Induced Fever and the Antipyretic Effects of Naproxen

Parameter	Unit	Estimate	RSE (%)	Inter-individual variability (%)
T_{ref}	°C	37.4	0.1	8
amp	–	0.013	8	29
$p_{HF,yeast}$	–	0.060	11	19
$p_{HF,drug}$	–	0.029	23	19
$k_{HF(same\ for\ yeast\ and\ drug)}$	h^{-1}	1.9	21	79
T_{LOW}	°C	35.1	1	2
a_1	–	0.16	4	–
a_2	–	0.15	10	21
b_1	–	0.018	21	48
b_2	–	0.19	20	48
k_p	h^{-1}	0.057	3	–
k_{out}	h^{-1}	2.0	2	1
I_{max}	–	0.042 fixed	–	–
IC_{50}	μM	40	5	30
n	–	3.1	2	–

Residual variability was 0.33 and 0.32, respectively.

Explanations of the symbols can be found in Eqs. 2, 4, 5, 7, and 8 in "Modeling of the Analgesic Effects."

RSE relative standard error of estimate

Pharmacokinetics

The time-course of naproxen was described by a two-compartment model. Half-life (3.5 h), *CL* (0.03 L/h/kg), and V_{ss} (0.17 L/kg) are in agreement with previously reported values (20–22). Naproxen clearance was reduced by 24% in animals with fever. Naproxen is mainly metabolized through glucuronidation (23,24). Fever has been reported before to reduce the proportion of drug transformed through glucuronidation for salicylamide and paracetamol (25,26), and this might therefore explain the observed reduction in *CL*.

Analgesic Effect

To study the analgesic effects of naproxen, monoarthritis was induced in an ankle joint by a carrageenan injection (16). This type of pain model has been used for over 30 years (14). As readout the guarding index was determined using the PawPrint method. This method is

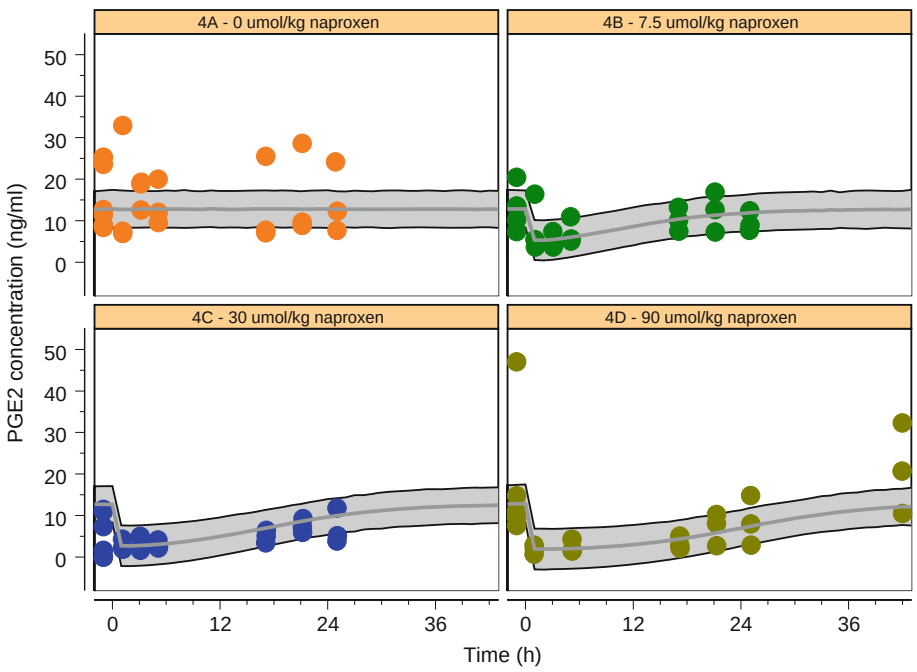

Fig. 6 Concentration of *ex vivo* synthesized PGE_2 after administration of Brewer's yeast or saline and oral dosing of 0, 7.5, 30, and 90 μmol/kg naproxen (time = 0 h). The data are from study 4. Individually observed concentrations are indicated with dots, the population predictions with a thick line, and the 95% prediction intervals after 1,000 simulations with thin lines.

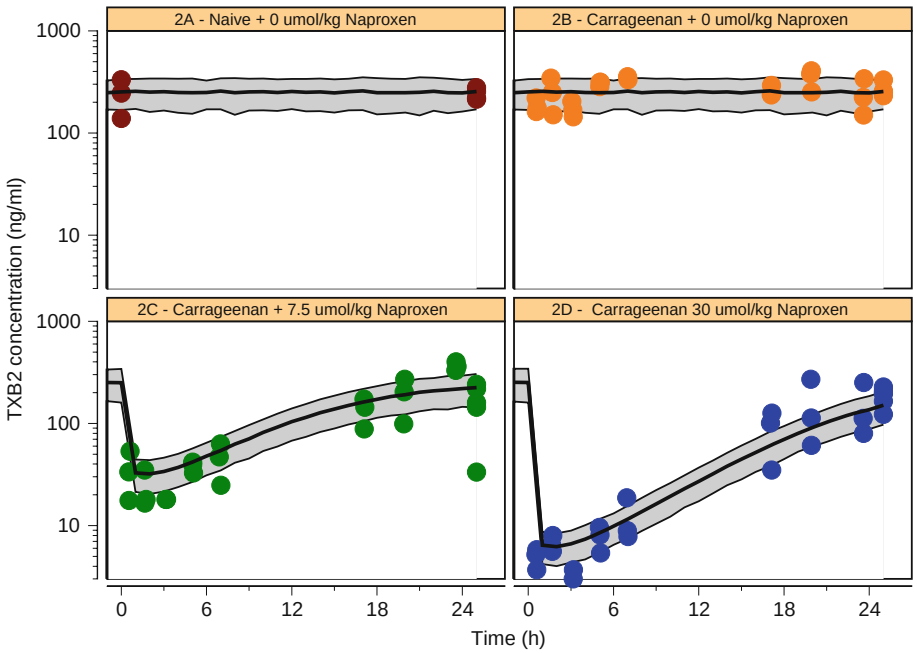

Fig. 7 Concentration of *ex vivo* synthesized TXB_2 after administration of carrageenan or saline (time = −1 h) and oral dosing of 0, 7.5, and 30 μmol/kg naproxen (time = 0 h). The data are from studies 1 and 2. Individually observed concentrations are indicated with dots, the population predictions with a thick line, and the 95% prediction intervals after 1,000 simulations with thin lines.

based on the concept of the CatWalk quantitative gait analysis technique, which has been validated as a behavioral method to quantify pain in rodent models of neuropathic and monoarthritic pain (15,16).

One obstacle in pain studies is the high variability between and within individual animals. Although a dose-dependent effect of naproxen appears to be present (Fig. 2), the variability made it difficult to identify a clear concentration-effect relationship and to identify the underlying time-dependent processes. It was necessary to estimate the time-course of the guarding index and drug effects in a two-step approach. The reported analgesic IC_{50} value (27 (0–130) μM) has a large uncertainty, and its 95% confidence interval includes several log units of concentration even though its range is similar to that reported previously (21).

The experimental design in study 1 also demonstrates that repeated measurements in an individual do not diminish overall variability. The large within-individual variability indicates that a larger number of individuals would be necessary per time-point to investigate the time-course and concentration-effect relationship properly. In addition, the carrageenan-induced increase in the guarding index is not constant over time due to the underlying dynamic inflammation process. For a compound with a half-life of several hours, such as naproxen, an animal model with a constant pain level might be more suitable for this type of investigation.

Antipyretic Effect

Brewers' yeast was used to induce fever to study the antipyretic effects of naproxen. Fever induced by brewers' yeast was reported to give fever lasting up to 30 h (13,27–29), whereas lipopolysaccharide (LPS) was reported to only give fever for up to 8 h (in-house observations, (27,30,31)). Having a long duration of fever made it possible to study a larger part of the time-effect profile of naproxen. The estimated potency of 40 (30–65) μM was in similar range as for the inhibition of LPS-induced fever (21).

Table V Population Pharmacodynamic Parameter Estimates for the Effects of Naproxen on the Inhibition of *ex vivo* TXB_2 and PGE_2 Synthesis

Parameter	Unit	Estimate	RSE (%)	Inter-individual variability (%)
$BM_{0,TXB2}$	$ng \cdot mL^{-1}$	251	5	–
$IC_{50,TXB2}$	μM	5.3	13	–
$I_{max,TXB2}$	$ng \cdot mL^{-1}$	1 (fixed)	–	–
n_{TXB2}	–	1.3	5	–
$BM_{0,PGE2}$	$ng \cdot mL^{-1}$	12.6	9	39
$IC_{50,PGE2}$	μM	13	29	38
$I_{max,PGE2}$	$ng \cdot mL^{-1}$	11.4	12	39
n_{PGE2}	–	1.0	25	–

Residual variabilities for TXB_2 and PGE_2 were 42% and 29%, respectively. Explanations of the symbols can be found in Eq. 2, in "Modeling of the Analgesic Effects."

RSE relative standard error of estimate

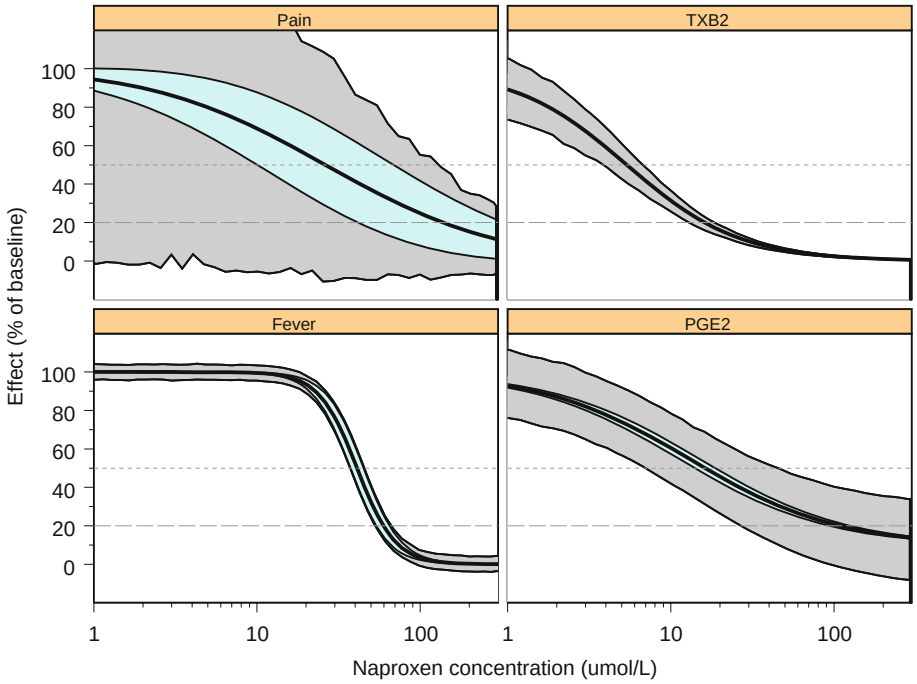

Fig. 8 Comparison of the naproxen effects on pain, fever, *ex vivo* TXB_2 synthesis, and *ex vivo* PGE_2 synthesis. Naproxen effects on all measurements were described by inhibitory sigmoidal equations, which express the drug effect as% of disease progression baseline. The 50% and 80% inhibition level for each biomarker are indicated by dotted reference lines. The light blue area indicates the confidence interval of the IC_{50} with inter-individual variability; the gray area indicates the confidence interval for the inter- and intra-individual variability combined.

Following naproxen administration, body temperature decreased initially; however, this decrease was followed by a rebound phase in which body temperature was higher than the fever (vehicle) profile. These observations were well described by a precursor-dependent indirect effect model (19). One physiological explanation for this observation could be that naproxen inhibits the COX enzymes, thereby reducing the formation of PGE_2 and other inflammatory mediators and subsequent fever (32–35). However, accumulated pro-inflammatory mediators could give rise to a new boost of PGE_2 and other inflammatory mediators when naproxen concentrations decrease, resulting in elevated body temperatures which are higher than body temperature in the control group. Alternatively, the highest dose (90 μmol/kg) could have induced GI-related side effects such as ulcerations that also could have been responsible for an increase in PGE_2 levels at later time points. The observation of this rebound phenomenon on fever has, to our knowledge, not been reported before and raises the question of whether similarities could be expected for other NSAIDs/COX-2 inhibitors and other endpoints such as the analgesic effects.

Time-Course of Pain and Fever

The time-course of the pain behavior and fever were similar in shape and could both be described by a Bateman function that was modified to allow for a delay in onset (17). Carrageenan and brewers' yeast are proinflammatory factors that cause an up-regulation of COX-2 (8,9), which in turn converts arachidonic acid into factors that mediate inflammation, pain and fever. Time is needed to convert the proinflammatory stimuli into pain- and fever-mediating factors through this cascade, which explains the delay in onset of the time-course of the guarding index and fever. The time to maximum elevated body temperature after yeast injection was approximately 4 h. It took 3 h after carrageenan injection to get a maximum increase in the guarding index, suggesting that it might be better to administer naproxen at least 3 h after carrageenan to avoid interference with underlying disease processes (36).

The Bateman function could also describe the initial hypothermic response after the injection of yeast. Biphasic fever responses to yeast or LPS have been observed before (29,30,37,38). Although it is still unclear what triggers the different phases, it could be due to involvement of thermoregulatory processes (30). The size of this hypothermic response has been also reported to be dependent on the time of day when fever is induced (28). It is also important to note that fever is regulated predominantly centrally and that it cannot be completely excluded that this marker could behave differently from down-stream COX-2 markers in the periphery due to pharmacokinetic distribution factors.

Inhibition of *Ex Vivo* Synthesis of the Biomarkers TXB_2 and PGE_2

The potency of naproxen, expressed as IC_{50} values, in inhibiting *ex vivo* TXB_2 and PGE_2 synthesis was 5 (4–8) μM and 13 (6–45) μM, respectively. No delay in the onset of inhibition was observed. This is in agreement with previous reports (20).

Comparison of *In Vivo* Markers and Translational Aspects

A two-fold difference was observed between COX-1 and COX-2 inhibition, indicating that naproxen is slightly COX-1 selective, which has been shown before (20,39,40). Naproxen was equipotent with respect to its analgesic and antipyretic effects and PGE_2 inhibition. Josa *et al.* also reported similar potency for analgesic and antipyretic effects (21). Usually, the IC_{50} value is the most commonly used parameter for potency; however, it has been suggested that, for the inhibition of *ex vivo* PGE_2 synthesis by NSAIDs, IC_{80} values is more relevant to predict clinical efficacy (11,39,40).

In humans, the therapeutic effective concentration is reported to be ~250 μM and correlates to the IC_{80} values for PGE_2 inhibition, which is reported in the range of 130–260 μM (11,39,40). In the present investigation, the IC_{80} for PGE_2 inhibition was 85 μM. This concentration resulted in significant analgesic and antipyretic effects, for which the IC_{80} were 134, 60 μM, respectively. The slight difference in IC_{80} values between rat and human might be explained by species differences in plasma protein binding (11,20).

The variability between individuals was considerably larger for the analgesic effects than for the other endpoints. This uncertainty could be reduced by increasing the number of animals per time-point, which could be difficult from ethical and resource perspectives. On other hand, the present investigation shows that the antipyretic effects and prostaglandin inhibition could serve as alternative endpoints to estimate the *in vivo* potency and time-course of analgesic drugs inhibiting the COX2 pathway for comparative and for translational purposes due to the possibility of repeated measurements and increased reproducibility and sensitivity. The *in vivo* pain model could in its turn be used to confirm the analgesic effects of the selected compounds to increase confidence in human dose predictions.

An important future data-analysis would be to analyze all data in a mechanism-based approach by modeling the analgesic effects and the antipyretic effects as functions of the observed PGE_2 inhibition. In such an analysis approach, the drug- and system-specific parameters can be derived, in which drug-specific parameters give information on the inhibition of PGE_2, and system-specific parameters give information on how the inhibition of PGE_2 leads to analgesic and antipyretic effects. Another advantage of such a mechanistic approach is that it could help to quantify if the inhibition of other targets in the COX-2 pathway would lead to a similar analgesic/antipyretic response as for NSAIDS, which is important for human dose predictions. However, such an analysis would require similar data of additional compounds in the PGE_2 assay and the analgesic and antipyretic animal models.

CONCLUSION

Naproxen was shown to inhibit the time-courses of pain, fever and PGE_2 with similar potencies (IC_{50}), but variability in the behavioral measurement of analgesia was larger than for the other endpoints. The time-courses for inflammatory pain and fever showed a delay in onset and a dynamic profile. The inhibition of fever by naproxen was followed by an increase (rebound) in body temperature compared to the vehicle profile. Due to the possibility of repeated measurements and increased reproducibility and sensitivity, the biomarker PGE_2 and the antipyretic effect would be suitable alternative endpoints for investigations and comparisons of the time-course and potency of various drug candidates in the COX-2 pathway and to support human dose projections.

ACKNOWLEDGMENTS

The authors thank Lars I. Andersson for help with TXB_2 & PGE_2 assays, Ulrika Määttä for assisting with biomarker sampling and Kristina Brunfelter, Sveinn Briem, Yvonne Jaksch, and Jonas Malmberg for help with the various bioanalyses.

REFERENCES

1. Whiteside GT, Adedoyin A, Leventhal L. Predictive validity of animal pain models? A comparison of the pharmacokinetic-pharmacodynamic relationship for pain drugs in rats and humans. Neuropharmacology. 2008;54(5):767–75.
2. Negus SS, Vanderah TW, Brandt MR, Bilsky EJ, Becerra L, Borsook D. Preclinical assessment of candidate analgesic drugs: recent advances and future challenges. J Pharmacol Exp Ther. 2006;319(2):507–14.
3. Mukherjee A, Hale VG, Borga O, Stein R. Predictability of the clinical potency of NSAIDs from the preclinical pharmacodynamics in rats. Inflamm Res. 1996;45(11):531–40.
4. Huntjens DR, Spalding DJ, Danhof M, Della Pasqua OE. Differences in the sensitivity of behavioural measures of pain to the selectivity of cyclo-oxygenase inhibitors. Eur J Pain. 2009;13(5):448–57.
5. Sultana SR, Roblin D, O'Connell D. Translational research in the pharmaceutical industry: from theory to reality. Drug Discov Today. 2007;12(9–10):419–25.
6. Colburn WA, Lee JW. Biomarkers, validation and pharmacokinetic-pharmacodynamic modelling. Clin Pharmacokinet. 2003;42(12):997–1022.
7. Vardeh D, Wang D, Costigan M, *et al.* COX2 in CNS neural cells mediates mechanical inflammatory pain hypersensitivity in mice. J Clin Invest. 2009;119(2):287–94.
8. Zhang Y, Shaffer A, Portanova J, Seibert K, Isakson PC. Inhibition of cyclooxygenase-2 rapidly reverses inflammatory hyperalgesia and prostaglandin E2 production. J Pharmacol Exp Ther. 1997;283(3):1069–75.
9. Seibert K, Zhang Y, Leahy K, *et al.* Pharmacological and biochemical demonstration of the role of cyclooxygenase 2 in

inflammation and pain. Proc Natl Acad Sci U S A. 1994;91 (25):12013–7.
10. Warner TD, Vojnovic I, Bishop-Bailey D, Mitchell JA. Influence of plasma protein on the potencies of inhibitors of cyclooxygenase-1 and -2. FASEB J. 2006;20(14):542–4.
11. Huntjens DR, Danhof M, Della Pasqua OE. Pharmacokinetic-pharmacodynamic correlations and biomarkers in the development of COX-2 inhibitors. Rheumatology (Oxford). 2005;44 (7):846–59.
12. Brideau C, Kargman S, Liu S, *et al.* A human whole blood assay for clinical evaluation of biochemical efficacy of cyclooxygenase inhibitors. Inflamm Res. 1996;45(2):68–74.
13. Tomazetti J, Avila DS, Ferreira AP, *et al.* Baker yeast-induced fever in young rats: characterization and validation of an animal model for antipyretics screening. J Neurosci Methods. 2005;147 (1):29–35.
14. Arrigoni-Martelli E. Screening and assessment of antiinflammatory drugs. Methods Find Exp Clin Pharmacol. 1979;1(3):157–77.
15. Vrinten DH, Hamers FF. 'CatWalk' automated quantitative gait analysis as a novel method to assess mechanical allodynia in the rat; a comparison with von Frey testing. Pain. 2003;102(1–2):203–9.
16. Angeby-Moller K, Berge OG, Hamers FP. Using the CatWalk method to assess weight-bearing and pain behaviour in walking rats with ankle joint monoarthritis induced by carrageenan: effects of morphine and rofecoxib. J Neurosci Methods. 2008;174(1):1–9.
17. Garrett ER. The Bateman function revisited: a critical reevaluation of the quantitative expressions to characterize concentrations in the one compartment body model as a function of time with first-order invasion and first-order elimination. J Pharmacokinet Biopharm. 1994;22(2):103–28.
18. Visser SA, Sallstrom B, Forsberg T, Peletier LA, Gabrielsson J. Modeling drug- and system-related changes in body temperature: application to clomethiazole-induced hypothermia, long-lasting tolerance development, and circadian rhythm in rats. J Pharmacol Exp Ther. 2006;317(1):209–19.
19. Sharma A, Ebling WF, Jusko WJ. Precursor-dependent indirect pharmacodynamic response model for tolerance and rebound phenomena. J Pharm Sci. 1998;87(12):1577–84.
20. Huntjens DR, Spalding DJ, Danhof M, Della Pasqua OE. Correlation between *in vitro* and *in vivo* concentration-effect relationships of naproxen in rats and healthy volunteers. Br J Pharmacol. 2006;148(4):396–404.
21. Josa M, Urizar JP, Rapado J, *et al.* Pharmacokinetic/pharmacodynamic modeling of antipyretic and anti-inflammatory effects of naproxen in the rat. J Pharmacol Exp Ther. 2001;297(1):198–205.
22. Runkel R, Chaplin M, Boost G, Segre E, Forchielli E. Absorption, distribution, metabolism, and excretion of naproxen in various laboratory animals and human subjects. J Pharm Sci. 1972;61(5):703–8.
23. Davies NM, Anderson KE. Clinical pharmacokinetics of naproxen. Clin Pharmacokinet. 1997;32(4):268–93.
24. Moyer S. Pharmacokinetics of naproxen sodium. Cephalalgia. 1986;6 Suppl 4:77–80.
25. Ismail S, Back DJ, Edwards G. The effect of malaria infection on 3′-azido-3′-deoxythymidine and paracetamol glucuronidation in rat liver microsomes. Biochem Pharmacol. 1992;44(9):1879–82.
26. Song CS, Gelb NA, Wolff SM. The influence of pyrogen-induced fever on salicylamide metabolism in man. J Clin Invest. 1972;51 (11):2959–66.
27. Santos FA, Rao VS. A study of the anti-pyretic effect of quinine, an alkaloid effective against cerebral malaria, on fever induced by bacterial endotoxin and yeast in rats. J Pharm Pharmacol. 1998;50(2):225–9.
28. Bruguerolle B, Roucoules X. Time-dependent changes in body temperature rhythm induced in rats by brewer's yeast injection. Chronobiol Int. 1994;11(3):180–6.
29. Refinetti R, Ma H, Satinoff E. Body temperature rhythms, cold tolerance, and fever in young and old rats of both genders. Exp Gerontol. 1990;25(6):533–43.
30. Dogan MD, Ataoglu H, Akarsu ES. Characterization of the hypothermic component of LPS-induced dual thermoregulatory response in rats. Pharmacol Biochem Behav. 2002;72(1–2):143–50.
31. Nakamura H, Mizushima Y, Seto Y, Motoyoshi S, Kadokawa T. Dexamethasone fails to produce antipyretic and analgesic actions in experimental animals. Agents Actions. 1985;16(6):542–7.
32. Blatteis CM. Endotoxic fever: new concepts of its regulation suggest new approaches to its management. Pharmacol Ther. 2006;111(1):194–223.
33. Steiner AA, Ivanov AI, Serrats J, *et al.* Cellular and molecular bases of the initiation of fever. PLoS Biol. 2006;4(9):e284.
34. Romanovsky AA, Almeida MC, Aronoff DM, *et al.* Fever and hypothermia in systemic inflammation: recent discoveries and revisions. Front Biosci. 2005;10:2193–216.
35. Ross G, Hubschle T, Pehl U, *et al.* Fever induction by localized subcutaneous inflammation in guinea pigs: the role of cytokines and prostaglandins. J Appl Physiol. 2003;94(4):1395–402.
36. Bueters TJ, Hoogstraate J, Visser SA. Correct assessment of new compounds using *in vivo* screening models can reduce false positives. Drug Discov Today. 2008;14(1–2):89–94.
37. Romanovsky AA, Kulchitsky VA, Simons CT, Sugimoto N. Methodology of fever research: why are polyphasic fevers often thought to be biphasic? Am J Physiol. 1998;275(1 Pt 2):R332–8.
38. Romanovsky AA, Blatteis CM. Biphasic fever: what triggers the second temperature rise? Am J Physiol. 1995;269(2 Pt 2):R280–6.
39. Capone ML, Tacconelli S, Sciulli MG, *et al.* Human pharmacology of naproxen sodium. J Pharmacol Exp Ther. 2007;322(2):453–60.
40. Warner TD, Guiliano F, Vojnovic I, Bukasa A, Mitchell JA. Nonsteroid drug selectivities for cyclo-oxygenase-1 rather than cyclo-oxygenase-2 are associated with human gastrointestinal toxicity: a full *in vitro* analysis. Proc Natl Acad Sci USA. 1999;96 (13):7563–8.